

Connect the Dots: Knowledge Graph-Guided Crawler Attack on Retrieval-Augmented Generation Systems

Mengyu Yao*, Ziqi Zhang†, Ning Luo†, Shaofei Li*, Yifeng Cai*, Xiangqun Chen*, Yao Guo* and Ding Li*

*Key Laboratory of High-Confidence Software Technologies (MOE), School of Computer Science, Peking University

†Department of Computer Science, University of Illinois Urbana-Champaign

Abstract—Retrieval-augmented generation (RAG) systems integrate document retrieval with large language models and have been widely adopted. However, in privacy-related scenarios (e.g., medical diagnosis), RAG introduces a new privacy risk: adversaries can issue carefully crafted queries to exfiltrate sensitive content from the underlying corpus gradually. Although recent studies have demonstrated multi-turn extraction attacks, they rely on heuristics and fail to perform long-term extraction planning. As a result, they typically stagnate after a few rounds and exfiltrate only a small fraction of the private corpus. To address these limitations, we formulate the RAG extraction attack as an adaptive stochastic coverage problem (ASCP). In ASCP, each query is treated as a probabilistic action that aims to maximize conditional marginal gain (CMG), enabling principled long-term planning under uncertainty. However, integrating ASCP with practical RAG attack faces three key challenges: unobservable CMG, intractability in the action space, and feasibility constraints. To overcome these challenges, we maintain a global attacker-side state to guide the attack. Building on this idea, we introduce RAGCRAWLER, which builds a knowledge graph to represent revealed information, uses this global state to estimate CMG, and plans queries in semantic space that target unretrieved regions. It also generates benign-looking prompts that elicit the remaining content while preserving stealth. In comprehensive experiments across diverse RAG architectures and datasets, our proposed method, RAGCRAWLER, consistently outperforms all baselines. It achieves up to 84.4% corpus coverage within a fixed query budget and deliver an average improvement of 20.7% over the top-performing baseline. It also maintains high semantic fidelity and strong content reconstruction accuracy with low attack cost. Crucially, RAGCRAWLER proves its robustness by maintaining effectiveness against advanced RAG systems employing query rewriting and multi-query retrieval strategies. Our work reveals significant security gaps and highlights the pressing need for stronger safeguards for RAG.

1. Introduction

Retrieval-Augmented Generation (RAG) has emerged as a powerful paradigm that integrates information retrieval with large language models (LLMs), allowing systems to dynamically access and utilize external knowledge bases

for tasks such as question answering, summarization, and decision support [1], [2]. By providing timely, domain-specific evidence beyond a model’s parametric memory, RAG has seen rapid adoption across settings ranging from enterprise knowledge management [3] to healthcare [4], and customer service [5].

RAG’s retrieval capabilities introduce significant privacy risks, as many of the data sources it accesses or stores contain confidential information. Recent studies demonstrate that sensitive data can leak from RAG by eliciting verbatim passages [6], [7], exposing personal identifiers from clinical notes or confidential clauses from internal documents. Such leaks can lead to non-compliance with GDPR and HIPAA [8], [9], resulting in legal, financial, and reputational harm [10]. Abusing the retrieval capabilities, adversaries can exploit the retriever as a high-precision oracle to exfiltrate private corpus content through carefully crafted prompts.

Understanding of the threat posed by extraction attacks on RAG remains limited, as existing studies often overlook adversaries’ global planning capabilities when crafting the prompts. In known attacks, prompts often build on recent responses, expanding on the retrieved context to uncover progressively more information. For example, an attack might extract a keyword from a recent answer and query it further [11], or instruct the LLM to elaborate on a just-mentioned fact [12]. These heuristic methods lack global planning and will often drift off topic (as shown in the left panel Fig. 1(a)) or re-touches previously seen content (as shown in the middle panel Fig. 1(a)), producing low-value responses and stalling early, leaving a substantial portion of the corpus remains unexplored as illustrated in Fig 1(b). Most importantly, while the empirical results demonstrate the feasibility of extracting content from RAG, the theoretical grounding and provable guarantees remain missing.

In this work, we provide theoretical guarantees for data extraction and systematical approach to analysis the extraction capability of practical adversaries. Our key insight is that these extraction attacks can be formalized as an instance of the **Adaptive Stochastic Coverage Problem (ASCP)** [13], [14], [15], where different attacks can be viewed as various strategies for solving the underlying coverage objective. ASCP is well studied in submodular optimization and the near-optimal strategy exists: if the coverage function, representing the fraction of the corpus revealed, is both adaptively monotone and adaptively submodular, then

a greedy policy that, at each step, selects the query with the largest conditional expected marginal gain (CMG) is a near-optimal strategy. In our formulation, each query is treated as an action that stochastically reveals a subset of hidden documents, and the objective is to maximize the expected corpus coverage given a limited query budget. Leveraging results from ASCP, we show that an attack on RAG, which globally plans queries to maximize CMG, can approach the theoretical upper bound on extracting RAG’s content.

Translating theoretical understanding into real-world attacks is challenging because of the following gaps that arise when instantiating the conditional margin gain (CMG), action space, and budget constraints of ASCP for RAG attacks: **❶ CMG of the attacker’s action is unobservable**: the attacker cannot directly measure the coverage increment produced by a query and subsequent retrievals, since they lack a global view of the document corpus. Consequently, the true CMG is *unobservable* and cannot be computed exactly. **❷ Attacker action spaces are intractable**: the query space Q is effectively unbounded (any natural-language string). Exhaustive search for the CMG-maximizing query is infeasible absent additional structure or strong priors. **❸ Defense of real-word RAG poses its own feasibility constraints**: queries in real-world RAG must remain natural and innocuous to avoid detection or refusal; high-gain intents must be expressed in policy-compliant surface forms that blend into ordinary usage. In addition, as real-world RAG systems often employ advanced query processing techniques such as query rewriting and multi-query retrieval, it becomes even more critical to articulate the intent explicitly to prevent the original meaning from being altered during these processes.

We propose a novel attack framework, RAGCRAWLER, to address these challenges. RAGCRAWLER maintains a structured attacker-side knowledge graph (KG) to give the attacker an overview of acquired information. With this global view, our attack executes a three-stage loop. First, KG construction utilizes existing answers and a coverage proxy to map graph growth to an estimate of coverage marginal gain, making it observable. Second, strategy scheduling replaces the intractable search with a two-stage selection process, driven by a score that fuses historical gain with structural exploration. Third, the query generation produces top-ranked anchors into natural, policy-compliant queries with history-aware deduplication. These three steps together act as an adaptive greedy coverage maximization strategy for RAGCRAWLER, which guarantees that RAGCRAWLER achieves near-optimal coverage of the RAG content.

To evaluate the effectiveness of RAGCRAWLER, we conduct a comprehensive evaluation across four benchmarks, four RAG generators (with safeguard variants), and two RAG retrievers. Results show that RAGCRAWLER consistently outperforms baselines in coverage rate, semantic fidelity, and reconstruction fidelity. RAGCRAWLER achieves an average coverage rate of 66.80%, which is a 20.70% improvement over the best baseline. Besides, the extracted content is of high quality, enabling the construction of a substitute RAG system that achieves a 0.6992 semantic similar-

ity to the original RAG’s responses. RAGCRAWLER maintains effective against generators with safeguards (reaching an average coverage rate of 55.30%) and potential defense mechanisms (including query rewriting and multi-query retrieval). In summary, our contributions are:

- We formalize data extraction attack in RAG as RAG Crawling, an adaptive stochastic coverage problem, and provide a rigorous theoretical foundation for the attack.
- We design RAGCRAWLER, a novel coverage-guided crawler that offers the provable near-optimal attack strategy under real-world constraints.
- We conduct extensive evaluations across diverse settings to demonstrate the effectiveness of RAGCRAWLER, as well as against modern RAG defenses.

2. A Motivating Example

Consider an attacker targeting a private medical corpus, as shown in Fig. 1(a). The corpus contains de-identified records (represented by 🚑, 🚒, and 🚑). The attacker engages the RAG system in a dialogue and gradually coaxes out sensitive medical facts about each individual via carefully crafted follow-up queries. Previous results already show that even after removing direct personal identifiers, inference attacks can still re-identify individuals and reveal sensitive attributes when sufficient information is obtained [16], [17], [18]. This scenario (though synthetic for illustration) reflects a real threat model: by asking seemingly innocuous questions in sequence, an attacker can piece together confidential information about different people from the underlying private database. As illustrated in Fig. 2, gaps in knowledge by identifying insufficiently covered areas can be detected by a knowledge graph and then used to generate targeted queries to fill those gaps, delving deeper into the sensitive medical facts related to each individual.

Existing work can be categorized into two types: continuation expansion and keyword expansion. In the first strategy (e.g., RAGThief [12]), the new query is built on the context of existing answers. The problem of this strategy is that the query can easily drift away from the actual corpus content. For example, in Fig. 1(a), the last answer reveals 🚑’s family medical history and mentions the baby’s grandfather 🚑. A continuation-based attacker will ask about the grandfather next, but since 🚑 is not in the corpus, this line of questioning yields no useful information. A keyword-based strategy (e.g., IKEA [11]) pivots each new query around key terms gleaned from previous answers, but the problem is that it tends to stay within the same semantic neighborhood of the corpus. For example, in Fig. 1(a), keyword-based attack repeatedly ask about 🚑’s disease and does not explore new topics.

Our work uses a **growing knowledge graph** to represent discovered entities and relations. A node represents an entity (e.g. a patient, a symptom), and edges capture relations or co-occurrences between entities (for example, patient → symptom if a patient is noted to have a certain symptom). As the attacker obtains new answers, the graph is expanded with any newly revealed entities or connections.

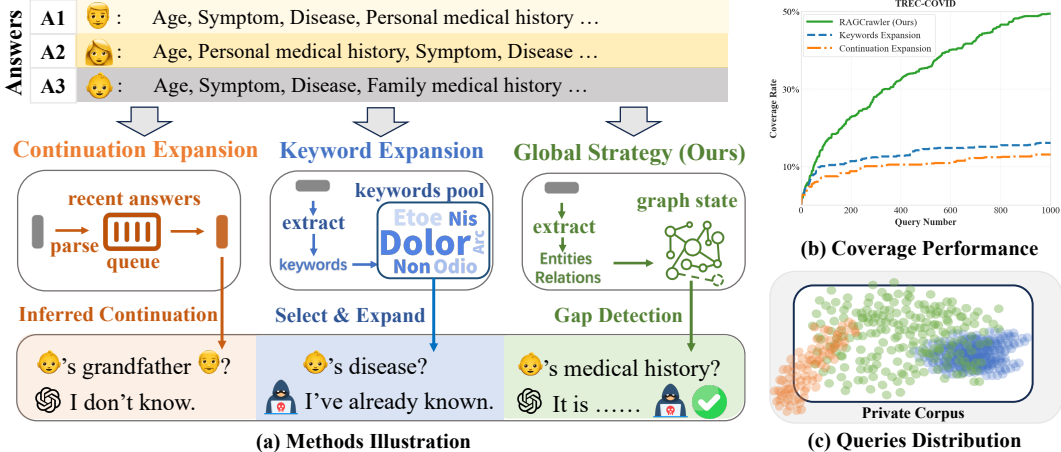


Figure 1: **A motivating example.** (a) A data extraction scenario on a private medical corpus. The continuation strategy follows the recent answer’s context, which can drift away from the corpus content; the keyword strategy reuses extracted keywords to form new queries, often yielding redundant information from the same semantic region; our proposed strategy maintains a global graph, detects unrevealed facts and targets them with new queries. (b) Knowledge coverage vs. query number for each strategy on the example corpus. (c) Distribution of retrieved facts in the corpus’ semantic space. Each point is a fact or document, with colors indicating queries from different strategies.

By maintaining this global knowledge state, the attacker can detect gaps in what has been revealed so far. As illustrated in Fig. 2, the knowledge graph dynamically reveals incomplete regions of information. For instance, the graph shows that the patient has no extracted *Personal Medical History*, while the other patients and already have their medical histories identified. Then the next query will be directed to the uncovered data of ’s unobserved medical history, and expanding overall coverage.

Fig. 1(b) shows the knowledge coverage rate v.s. the number of queries for our attack and two baseline strategies. Guided by the global knowledge graph, our attack (green line) achieves a much steeper increase in coverage compared to the continuation-based (orange curve; focusing on unrelated queries) and keyword-based (blue curve; focusing on repetitive queries) strategies.

Fig. 1(c) provides a qualitative view of how each strategy explores the semantic space of the corpus. In this visualization, each point represents a distinct fact or document. The color represents the strategy that retrieves the document. The black box represents the space of the private corpus. We can observe that, guided by the global knowledge graph, our attack spread widely across the private space and covers

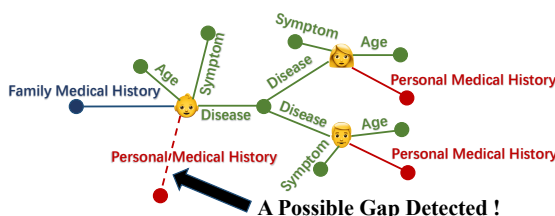


Figure 2: **Illustration of gap detection by the Global Strategy (Ours).** The strategy identifies from the graph that the patient has a missing *Personal Medical History*, and guides the next exploration step to complete the knowledge.

many different clusters of information. The continuation-based queries (orange points) follow a narrow path through the space, gradually drifting away from the space center. The keyword-based queries (blue points) form a few dense clusters around specific anchor topics.

3. Background

In this section, we introduce the background, including Retrieval-Augmented Generation Systems (Sec. 3.1), Adaptive Stochastic Coverage Problem (Sec. 3.2) and Knowledge Graph (Sec. 3.3).

3.1. Retrieval-Augmented Generation Systems

A Retrieval-Augmented Generation (RAG) system \mathcal{S} typically comprises a generator \mathcal{G} (an LLM), a retriever \mathcal{R} , and a document collection \mathcal{D} . Given a user query q , the retriever \mathcal{R} begins by producing an embedding for q and based on some similarity function (typically cosine similarity), fetching the k most relevant documents:

$$\mathcal{D}_k(q) = \arg \text{top-}k_{d \in \mathcal{D}} \text{sim}(q, d). \quad (1)$$

where $\text{sim}(\cdot)$ represents the similarity function, and $\arg \text{top-}k$ selects the top- k documents with the highest similarity scores. The generator \mathcal{G} then generates an output based on the contextual information from the retrieved documents. The generator then produces an answer conditioned on the query and retrieved context [2]:

$$a = \mathcal{G}(\text{wrapper}(q, \mathcal{D}_k(q))), \quad (2)$$

where $\text{wrapper}(\cdot, \cdot)$ denotes the system prompt that interleaves q with the retrieved evidence.

In practice, deployed RAG pipelines often incorporate guardrails or enhancements. The most commonly used are *query rewriting* and *multi-query retriever*.

Query rewriting [19], [20], [21], [22] transforms the original query to improve retrievability, resolve ambiguity, repair typos, or strip unsafe instructions. The downstream retrieval and generation processes then operate on the rewritten query. **Multi-query retrieval** [23], [24] generates multiple paraphrases of the original query and performs independent retrieval for each. The retrieved results are then aggregated into a candidate pool. Instead of concatenating all retrieved documents, RAG systems typically re-rank them to select the most relevant ones, with *Reciprocal Rank Fusion (RRF)* [25] being a widely adopted method. Multi-query retrieval is not a dedicated defense, but its altered retrieval dynamics may affect the attack surface.

3.2. Adaptive Stochastic Coverage Problem

The Adaptive Stochastic Coverage Problem (ASCP) considers scenarios in which each action reveals information in a stochastic manner, and subsequent decisions depend on the observations made so far. In this setting, each action corresponds to selecting a set whose information coverage is uncertain until it is executed. The coverage outcome of the same item can vary depending on the results of previously chosen actions. The objective is to maximize the overall information coverage within limited budgets, such as a limited number of actions.

An ASCP specification can formally be specified using item universe \mathcal{U} , action space \mathcal{Q} , stochastic query outcome $O(q)$, cost and budget $c(q), B$, and coverage function $f(S)$

- **Item universe (\mathcal{U}):** The item universe \mathcal{U} represents the set of all items that are available for coverage. These items are the targets for the actions, and the goal is to maximize coverage across this universe.
- **Action space (\mathcal{Q}):** The action space \mathcal{Q} consists of all possible actions that can be taken. Each action q corresponds to covering a set of items, but the outcome of this action is uncertain until it is executed.
- **Stochastic query outcome ($O(q)$):** The stochastic query outcome $O(q)$ defines the uncertain result of executing action q . It captures the probabilistic nature of the outcome, reflecting how the coverage outcome can vary depending on prior actions.
- **Cost and budget ($c(q), B$):** The cost $c(q)$ represents the resources required to perform action q , and B is the total available budget. The objective is to maximize coverage while staying within the budget constraint.
- **Coverage function ($f(S)$):** The coverage function $f(S)$ quantifies the total information coverage achieved by a set of actions S . It reflects the degree to which the selected actions have covered items from the item universe \mathcal{U} .

Theorem 1 (Approximation guarantee of adaptive greedy [13], [14], [15], [26], [27]). *Let f be the coverage function in an instance of the ASCP. Assume that f is adaptively monotone and adaptively submodular, meaning that taking more actions never reduces expected coverage and that each additional action yields diminishing returns. Let π_{greedy} be the adaptive greedy policy that, at each step, selects the action with the most significant conditional*

expected marginal gain, and let π^ be an optimal adaptive policy under the same number of actions. Then, the adaptive greedy policy π_{greedy} achieves the approximately optimal expected coverage¹ under a fixed action budget.*

We reduce the data extraction attack against RAG systems, which we term RAG Crawling to the ASCP to guide our solution (see Sec. 5).

3.3. Knowledge Graph

Knowledge graph (KG) is a widely-used knowledge representation technology to organize huge amounts of scattered data into structured knowledge. Formally, a KG is a directed, labeled graph $\mathcal{G} = (\mathcal{E}, \mathcal{L}, \mathcal{R})$, where \mathcal{E} is the set of entities, \mathcal{R} is the set of relation types (edge labels), and $\mathcal{L} \subseteq \mathcal{E} \times \mathcal{R} \times \mathcal{E}$ is the set of labeled, directed edges (facts). Each edge $l \in \mathcal{L}$ is a triple (h, r, t) that connects head $h \in \mathcal{E}$ to tail $t \in \mathcal{E}$ via relation $r \in \mathcal{R}$. For example, (Python, `instanceOf`, Programming Language).

Compared with unstructured text, KGs provide schema-aware, canonicalized facts with explicit connectivity and constraints [28]. We leverage the knowledge graph to construct an attacker-side state that makes coverage estimable, constrains exploration to a compact semantic action space, and records provenance for robust, auditable updates.

4. Threat Model

Scenario. As illustrated in Fig. 3, we consider a production RAG service accessed through a black box interface such as an API or chat. Internally, a retriever selects passages or documents from a private corpus \mathcal{D} and a generator composes an answer from the query and the retrieved evidence [1], [2]. In deployment the generator may rewrite, summarize, or refuse according to guardrails and access policies [23], [29]. The service does not reveal retrieval scores or document identifiers. The attacker has no insider access and interacts as a normal user. The attacker aims to extract as much of \mathcal{D} as possible while remaining unnoticed by steering retrieval to cover new items across turns.

Prior work has identified two broad classes of such extraction attacks in RAG systems: *Explicit* attacks append overt adversarial instructions to elicit verbatim disclosure of retrieved text [6], [12], [30], [31]. *Implicit* attacks use benign-looking queries and aggregate factual content that the system legitimately returns across turns, reconstructing private material via paraphrases and fragments [11]. Our focus is the implicit regime, which better matches real usage and evades straightforward refusal rules.

Adversary’s Goal. The attacker aims to exfiltrate the private knowledge base \mathcal{D} as completely as possible while avoiding detection. Leakage may appear as verbatim text, paraphrases, summaries, or factual statements that reflect retrieved evidence. For each round t , the adversary submits a query q_t . In response, the RAG system internally consults a

1. $(1 - 1/e) \approx 0.63$, i.e., greedy attains at least this fraction of the optimal expected coverage.

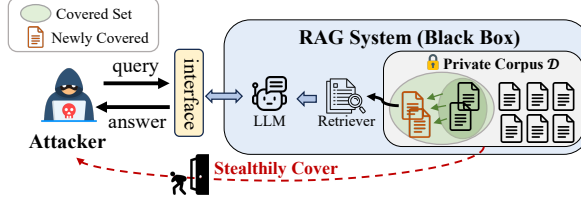


Figure 3: **Threat model of RAG Crawling.** An external attacker interacts with a production RAG system only via the public interface. For each query, the retriever selects a set of documents from the private corpus and the LLM generates an answer conditioned on this evidence. Across turns, the attacker aims to stealthily expand the union of leaked retrieved items under a query budget.

hidden set of documents $\mathcal{D}_k(q_t) \subseteq \mathcal{D}$ to generate its answer. The adversary’s goal is to maximize the number of unique documents retrieved over a sequence of B queries, thereby learning about the system’s underlying knowledge base. This budget B models real-world constraints such as API costs and the need to evade detection. This objective is formally expressed as the following:

$$\max_{\{q_1, \dots, q_B\}} \frac{|\bigcup_{t=1}^B \mathcal{D}_k(q_t)|}{|\mathcal{D}|} \quad (3)$$

Stealth remains a parallel objective: each q_t should look natural and innocuous to avoid detection or refusal.

Adversary’s Capabilities. We assume a black box setting. The attacker submits adaptive natural language queries q_t and observes only final answers a_t . They cannot see retrieval scores, document identifiers, or intermediate states, and they cannot read internal indices or modify retriever weights. They do not poison the target corpus and do not use privileged operator tools. Following prior work [11], [12], [30], the attacker knows only the topic of the target knowledge base, such as a keyword or short phrase that can be inferred from public materials or light probing. Under these constraints, leverage comes solely from crafting query sequences and interpreting observed answers.

5. Reducing RAG Crawling to ASCP

We now explain how we model the data extraction in RAG, RAG Crawling, as ASCP (introduced in Sec. 3.2). This formal mapping clarifies how we can potentially apply the greedy coverage-maximizing approach in our setting:

- **Item universe (\mathcal{U}):** We take \mathcal{U} to be the set of atomic documents or passages in the private corpus \mathcal{D} . Essentially, the “items” to be covered are the documents in \mathcal{D} .
- **Action space (\mathcal{Q}):** We equate the set of possible actions \mathcal{Q} with the set of all valid queries the attacker could ask might pose. In theory \mathcal{Q} is infinite (any string could be a query), but we will address how to search it later. For now, conceptually, each $q \in \mathcal{Q}$ is a possible question the attacker can pose to the target system.
- **Stochastic query outcome (Φ):** When the attacker issues a particular query q , the RAG system will retrieve some

set of documents $\mathcal{D}_k(q) \subset \mathcal{D}$ (Sec. 3.1) and then produce an answer. We model this retrieval result as a random subset drawn from a distribution $\Phi(\cdot | q)$. Essentially, Φ encapsulates our uncertainty about what part of \mathcal{D} will be exposed by query q .

- **Cost and budget:** We assume each query has a unit cost (e.g., each question counts as 1 against the budget B). This is a reasonable simplification: perhaps some queries could be considered “more costly” if they are longer or trigger more computation, but in our threat model the primary cost is just the opportunity cost of using up one of the limited queries we can send. Thus, a budget B simply means the attacker is limited to B queries in total.
- **Coverage function:** We define $f(S, \Phi)$ as the fraction of unique documents in \mathcal{D} that have been retrieved at least once by the set of queries S . Since the attacker cannot directly observe $\mathcal{D}_k(q)$, this is a latent coverage measure.

Under this reduction, the attacker is effectively an adaptive agent who, at each step $t = 1, 2, \dots, B$, selects a query $q_t \in \mathcal{Q}$ based on the interaction history so far, aiming to maximize the overall expected coverage $f(S, \Phi)$ by the end of B queries.

We now define the notion of adaptive marginal gain under the RAG Crawling model and show that it satisfies the core assumptions required for approximate greedy optimization in ASCP.

Definition 1 (Conditional Marginal Gain in RAG Crawling). *Let $S = \{q_1, \dots, q_t\}$ denote the set of queries issued so far, and let ψ denote the observable interaction history, that is, the sequence of issued queries and their corresponding observable system responses such as generated answers. Let Φ represent the underlying stochastic retrieval process that maps queries to latent sets of retrieved documents. The conditional marginal gain of issuing a new query $q \in \mathcal{Q}$ given history ψ is defined as*

$$\Delta(q | \psi) := \mathbb{E}_\Phi [f(S \cup \{q\}, \Phi) - f(S, \Phi) | \psi], \quad (4)$$

Theorem 2 (Adaptive Monotonicity and Submodularity in RAG Crawling). *The RAG Crawling problem instance satisfies adaptive monotonicity and adaptive submodularity.*

The proof can be found in Appendix 9.2. Building on Theorem 1 and Theorem 2, we have the following:

Theorem 3 (Near-optimality guarantee of RAGCRAWLER). *The adaptive greedy policy for RAG Crawling, which at each step t selects a query*

$$q_t \in \arg \max_{q \in \mathcal{Q}} \Delta(q | \psi_{t-1}), \quad (5)$$

achieves an approximately optimal expected coverage.

While this theorem provides a principled optimization target, implementing an adaptive greedy strategy in practice is far from trivial. Several challenges arise when translating the theoretical ASCP framework into a practical attack against real-world RAG systems:

- ❶ **The CMG is unobservable.** The attacker cannot directly observe the true coverage gain of a query, as the retrieved document sets remain hidden and inaccessible.
- ❷ **The attacker’s action space is intractable.** The action space \mathcal{Q} includes all valid natural language strings, making it effectively infinite. Without additional structure or priors, exhaustive search for high-gain queries becomes computationally infeasible.
- ❸ **Real-world RAG systems’s defense.** Queries must appear natural and comply with safety policies to avoid refusal, rejection, or detection by safety filters.

In next section, we explain how RAGCRAWLER, a black-box crawling framework designed, reconstructs the latent knowledge base of a RAG system under a fixed query budget. Grounded in the Adaptive Stochastic Coverage Problem (ASCP) formulation, RAGCRAWLER approximates the theoretical greedy coverage-maximization strategy by maintaining an evolving knowledge-graph state, identifying high-gain anchors in the semantic space of this state, and realizing them through stealthy queries.

5.1. Overview

In this section, we explain the operational workflow of RAGCRAWLER, illustrated in Fig. 4. The attacker begins by issuing an initial query q_0 to the victim RAG system and receiving the corresponding response a_0 . Upon receiving a query, the RAG retrieves a hidden set of documents from its private corpus and synthesizes an answer based on the retrieved evidence. Although the retrieved content is not directly observable, the generated response inevitably reveals partial fragments of the underlying corpus. The **KG-Constructor** module parses a_0 into structured triples and integrates them into the initial attacker-side KG \mathcal{G}_0 , which serves as an observable approximation of the latent corpus coverage. Based on this state, the **Strategy Scheduler** estimates the CMG over candidate entity-relation anchors in \mathcal{G}_0 , selects the most promising anchor Anc_0 , and forwards it to the **Query Generator**. The **Query Generator** realizes this anchor as a fluent and policy-compliant query q_1 , which is then sent to the RAG system to obtain the next response a_1 . The new answer a_1 is subsequently processed by the **KG-Constructor** to update the knowledge graph to \mathcal{G}_1 . Generalizing this process, at iteration t the attacker issues q_t , receives a_t , and updates the state \mathcal{G}_t through the same sequence of modules, forming a closed adaptive loop of *state estimation, strategic planning, and query realization*.

This adaptive loop systematically addresses the three challenges of the ASCP framework. Next, we elaborate on the specific mechanisms employed for each challenge.

5.2. KG-Constructor

This module addresses the first challenge in the ASCP formulation: *the CMG of the attacker’s action is unobservable*. Since the attacker cannot directly observe which documents have been retrieved by the RAG system, the true coverage increment of each query remains hidden. The

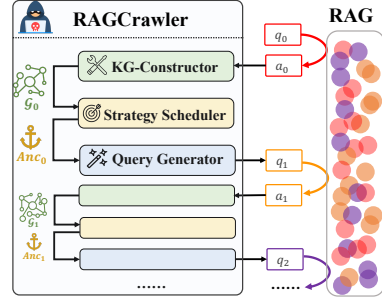


Figure 4: **The workflow of RAGCRAWLER.** At each step, (1) The KG-Constructor processes the latest system response to update the knowledge graph. (2) The Strategy Scheduler analyzes this graph to select a strategic anchor. (3) The Query Generator then uses this anchor to formulate the next query, completing the loop.

goal of this module is therefore to construct and maintain an evolving KG \mathcal{G}_t that approximates the latent coverage function $f(S^\pi, \Phi)$, making CMG estimable from surface-level answers. The workflow is shown in Fig. 5.

Why existing approaches do not work. Existing KG construction methods are ill-suited for our dynamic setting. Traditional techniques such as OpenIE and schema-constrained extraction [32], [33], rely on fixed relation inventories and curated ontologies, assuming stable data access and consistent syntax. Recent LLM-based approaches [34], [35] show promise for adaptive graph construction but conflicts with the need for efficient incremental updates that do not require full access to the underlying data. Furthermore, graph-augmented RAG frameworks such as GraphRAG [36] and LightRAG [37] use LLMs to extract triples from documents within the corpus and leverage the graph to enhance retrieval. These frameworks primarily focus on optimizing retrieval quality by merging exactly identical entities and relations. While this improves retrieval efficiency, it neglects the need for compact and efficient coverage tracking across multiple rounds of dynamic query responses.

Our methods. We develop a KG-Constructor that emphasizes efficient incremental updates. Instead of requiring access to the entire dataset or repeatedly rebuilding the global graph, we maintain the KG in a lightweight manner by constructing a subgraph at each step and merging it into the existing graph. As illustrated in Fig. 5, the workflow consists of three main modules:

1) Topic-Specific Prior. We begin by establishing a topic-specific prior that defines the contextual focus of the constructed KG. This prior acts as a soft constraint on the LLM’s extraction process, guiding it toward topic-relevant entities and relations while filtering out off-topic or noisy content. By narrowing the semantic search space, it enables more targeted and consistent knowledge acquisition. Concretely, we prompt the LLM to infer a compact set of entity categories and relation types that characterize the target domain. For example, in a medical corpus, entity categories may include *disease*, *symptom*, and *treatment*, while relation types may include *has_symptom*, *treated_by*,

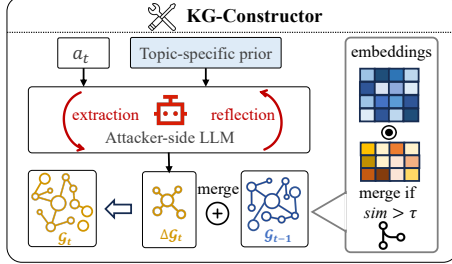


Figure 5: **The workflow of KG-Constructor.** Guided by a Topic-Specific Prior, an Iterative Extraction and Reflection process generates a knowledge subgraph ($\Delta\mathcal{G}_t$), which is then refined through Incremental Graph Update and Semantic Merging to produce the final graph state, \mathcal{G}_t .

and *caused_by*. During extraction, the LLM is instructed to prioritize these schema elements when forming structured triples, ensuring that all generated relations remain within the topical boundary. This bounded, schema-guided design offers two key advantages. First, it stabilizes relation typing and prevents the introduction of spurious or semantically inconsistent edges, maintaining structural coherence across incremental updates. Second, it keeps the prompt context compact and computationally efficient: the LLM does not need to reference all existing nodes and relations in the graph, but only the abstract schema of entity and relation types as contextual constraints. This design greatly reduces prompting overhead, enabling scalable LLM calls while preserving high topical precision in the extracted knowledge.

2) Iterative Extraction and Reflection. This component uses the attacker-side LLM to process the new answer. To reduce missing edges caused by conservative extraction, we adopt a multi-round extraction–reflection procedure. As shown in Fig. 5, each answer is first processed by an “extraction” pass, and then reprocessed through a “reflection” pass that revisits the same content with awareness of previously omitted facts. This reflection loop enables the LLM to infer implicitly expressed relations and produce additional triples, forming a more comprehensive knowledge subgraph $\Delta\mathcal{G}_t$.

3) Incremental Graph Update and Semantic Merging. After obtaining the new knowledge subgraph $\Delta\mathcal{G}_t$, it is incrementally integrated with the existing graph \mathcal{G}_{t-1} to form the updated graph \mathcal{G}_t . This integration is implemented as a lightweight merging operation without rebuilding graph from scratch. To ensure that the graph structure reflects genuine semantic expansion rather than redundant surface-level variations, we perform a semantic merging stage offline. All entity mentions and relation phrases are encoded into a shared embedding space using a pre-trained encoder. Node or edge pairs whose cosine similarity exceeds a threshold τ are automatically identified and merged. This joint reconciliation of entities and relations consolidates semantically equivalent concepts, normalizes synonymy across updates, and maintains a compact yet expressive knowledge graph. This provides a stable basis for CMG estimation and planning space for Strategy Scheduler (Sec. 5.3).

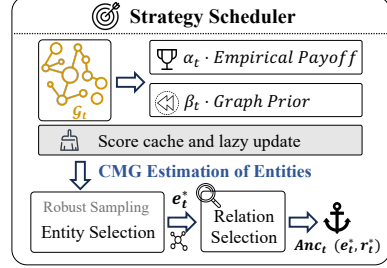


Figure 6: **The workflow of Strategy Scheduler.** The scheduler selects an action from the graph \mathcal{G}_t via a two-stage process. First, it samples an entity (e_t^*) based on a score that estimates CMG by balancing two key metrics. Second, it selects a relation (r_t^*) by identifying the entity’s largest local information deficit. A score cache with lazy updates ensures the efficiency of this process.

5.3. Strategy Scheduler

This module address the second challenge of the ASCP framework: *attacker action spaces are intractable*. Operating on the knowledge graph from the KG-Constructor, its task is to select the optimal entity-relation pair (e.g., (👉, *Family Medical History*)) to guide the next query. The primary difficulty is that the space of potential strategic actions is combinatorially vast, rendering a brute-force search for the optimal pair computationally infeasible. Our key insight is an asymmetry between entities and relations: entities are the primary drivers of coverage expansion, while relations refine the exploration direction. Exploiting this asymmetry, we reframe the problem into a hierarchical two-stage decision: first select an entity, then pick which of its unexplored relations to probe. The workflow is shown in Fig. 6.

Entities Selection. To identify the entity that maximizes expected coverage, RAGCRAWLER first estimate the CMG of each entity in \mathcal{G}_t using two complementary metrics: *empirical payoff* and *graph prior*. The *empirical payoff* captures historical information gain and reflects how informative an entity has been in past queries. The *graph prior* exploits the topology of the knowledge graph to identify entities located in structurally under-explored regions. By jointly capturing exploitation through past utility and exploration through structural potential, these metrics provide a more complete CMG estimation. Their values are combined via a dynamically weighted sum to produce a final score for each entity, and the anchor entity e_t^* is selected using robust Top-K softmax sampling.

Empirical payoff. We define the empirical payoff of an entity e via an upper-confidence style score:

$$\text{EmpiricalPayoff}(e) = \bar{g}_e + c\sqrt{\frac{\log N}{n_e + 1}}, \quad (6)$$

where \bar{g}_e is the empirical information gain of e , n_e is the number of times e has been selected as the anchor, N is the total number of anchor selections, and $c > 0$ controls the strength of the confidence bonus.

The first term \bar{g}_e estimates the contribution of e to past knowledge-graph expansion. It is calculated as the

normalized average increase in newly discovered entities and relations within a sliding window t_w :

$$\bar{g}_e = \frac{1}{n_e} \sum_{i \in \mathcal{I}(e)} \left(\underbrace{\Delta \mathcal{E}_i / \max(\Delta \mathcal{E}_{t_w})}_{\text{normalized new entities}} + \underbrace{\Delta \mathcal{R}_i / \max(\Delta \mathcal{R}_{t_w})}_{\text{normalized new relations}} \right), \quad (7)$$

where $\mathcal{I}(e)$ denotes the set of rounds where e served as the anchor, and $\Delta \mathcal{E}_i$ and $\Delta \mathcal{R}_i$ represent the newly discovered entities and relations in round i .

The second component is an exploration bonus, rooted in the “optimism in the face of uncertainty” principle from multi-armed bandit literature [38], [39]. This term adds a confidence-based reward that encourages the agent to visit less-frequently selected entities, thereby mitigating the risk of converging to a local optimum.

Graph prior. While the *empirical payoff* provides a self-contained mechanism for balancing exploitation and statistical exploration, it remains blind to the underlying topology of the knowledge graph. To overcome this limitation, we introduce a complementary, structure-aware exploration term: the *graph prior*. This prior injects topological intelligence into the strategy, directing it toward graph regions with high discovery potential. It is composed of two distinct terms:

$$\text{GraphPrior}(e) = \text{DegreeScore}(e) + \text{AdjScore}(e). \quad (8)$$

The first term, *DegreeScore*, promotes exploration in less-dense regions. It penalizes highly connected entities, operating on the intuition that these “hub” nodes are more likely to be information-saturated:

$$\text{DegreeScore}(e) = 1 - \frac{\deg(e)}{\max_{u \in \mathcal{E}} \deg(u) + \epsilon}. \quad (9)$$

The second term, *AdjScore*, directly measures an entity’s relational deficit. This deficit quantifies how common a specific relation type is among an entity’s peers, given that the entity itself lacks that relation. A high *AdjScore* thus signals a significant discovery opportunity, prioritizing entities that are most likely to form a new, expected type of connection:

$$\text{AdjScore}(e) = \max_{r \in \mathcal{R}} \text{Deficit}(e, r), \quad (10)$$

where the deficit for a specific relation r is defined as:

$$\text{Deficit}(e, r) = \begin{cases} 0, & \text{if } r \in \text{EdgeType}(e), \\ \frac{1}{|\mathcal{E}_{e.\text{type}}|} \sum_{u \in \mathcal{E}_{e.\text{type}}} \#\text{Edge}(u, r), & \text{if } r \notin \text{EdgeType}(e). \end{cases} \quad (11)$$

Here, $\text{EdgeType}(e)$ is the set of relation types already connected to e , and $\mathcal{E}_{e.\text{type}}$ is the set of all entities sharing the same semantic type as e .

Entity scoring and sampling. We integrate *empirical payoff* and *graph prior* into a final composite score. Critically, their relative importance may change over the course of an attack. We therefore combine them using time-varying weights

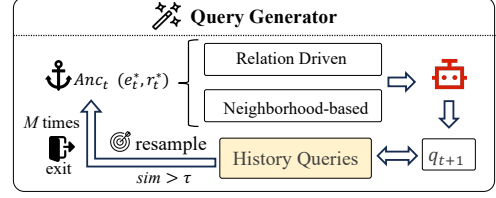


Figure 7: **The workflow of Query Generator.** It receives an anchor pair (e_t^*, r_t^*) and selects a generation strategy. A candidate query q_{t+1} is produced and checked against historical queries. If too similar, the generator requests a new anchor from the scheduler and resamples.

to enable dynamic control of the exploration-exploitation balance:

$$\text{Score}(e) = \alpha_t \cdot \text{EmpiricalPayoff}(e) + \beta_t \cdot \text{GraphPrior}(e), \quad (12)$$

where α_t gradually increases with time step t to favor high-confidence anchors in later stages, while β_t remains positive to maintain structural awareness.

Finally, to mitigate the risk of prematurely converging on a single, seemingly optimal path due to noisy gain estimates, we avoid a deterministic argmax selection. Instead, we sample the anchor entity e_t^* from a Top- K softmax distribution over the candidate scores, promoting strategic diversity and enhancing robustness.

Relation Selection. Given the sampled anchor e_t^* , we choose a relation by probing its largest local deficit:

$$r^*(e_t^*) = \arg \max_{r \in \mathcal{R} \setminus \text{EdgeType}(e_t^*)} \text{Deficit}(e_t^*, r). \quad (13)$$

To focus on meaningfully large gaps, we compare this maximum to the global distribution of current deficits,

$$\mathcal{DS}_t = \{ \text{Deficit}(e, r) : e \in \mathcal{E}_t, r \in \mathcal{R} \setminus \text{EdgeType}(e) \}, \quad (14)$$

and set $r_t^* = r^*(e_t^*)$ only if it exceeds the 90th percentile of \mathcal{DS}_t ; otherwise, we set $r_t^* = \emptyset$ to indicate that no single relation is a sufficiently promising target.

Ultimately, the scheduler outputs the pair (e_t^*, r_t^*) , which provides structured guidance to Query Generator (Sec. 5.4).

Optimization. To ensure scalability, the scheduler employs a lightweight caching mechanism. Previously computed $\text{Score}(e)$ values are stored in a score cache. Following an update to the knowledge graph \mathcal{G}_t , a lazy-update strategy is triggered: only the scores of entities directly affected by the changes are invalidated and recomputed. The scores for all unaffected entities are served directly from the cache. This approach decouples the computational cost of the scheduling step from the total size of the graph, ensuring that the decision loop remains efficient even as the attacker’s graph expands significantly.

5.4. Query Generator

This module addresses the third challenge in the ASCP formulation: *Real-world RAG systems impose practical constraints.* We cannot directly send a structured anchor (e_t^*, r_t^*)

to the system, and relying solely on simple templates is not a viable solution, as it can easily be flagged by query provenance mechanisms. Therefore, the core task of this module is to translate the abstract, strategic anchor pair from the Strategy Scheduler into a concrete, executable, and natural-sounding query q_{t+1} . This process must address two primary challenges: 1) generating a query that is contextually relevant to the anchor’s strategic intent, and 2) ensuring the query remains novel to avoid redundancy and maximize the utility of the limited query budget.

To achieve this, the generator involves three key steps: 1) adaptive query formulation, 2) history-aware de-duplication, and 3) a feedback mechanism for system-level learning. The workflow is shown in Fig. 7.

1) Adaptive Query Formulation. The generator’s first step is to intelligently select a formulation strategy based on the specificity of the anchor (e_t^*, r_t^*) provided by the scheduler. This dual-mode approach allows the system to flexibly switch between precision and discovery:

- **Relation-Driven Probing.** When the Strategy Scheduler identifies a plausible relation deficit r_t^* for an entity e_t^* with high confidence, the generator activates this targeted strategy. It instantiates a relation-aware template conditioned on the (e_t^*, r_t^*) pair and realizes it via an LLM into a fluent, natural language query q_{t+1} designed for precise fact-probing.
- **Neighborhood-based Generation.** In the absence of a sufficiently salient relation, the generator shifts to an exploratory mode. It analyzes the local neighborhood of e_t^* within the current knowledge graph \mathcal{G}_t . By leveraging the KG’s schema and the generative capabilities of LLM, it hypothesizes plausible missing relations and formulates one or more exploratory query variants.

2) History-aware De-duplication To maximize the information yield of each query, we introduce a robust quality control gate powered by a history-aware resampling loop. Before being dispatched, each candidate query q is compared against the historical query log $\mathcal{Q}_{\text{hist}}$. If its similarity $\text{sim}(q, \mathcal{Q}_{\text{hist}}) \geq \tau$, the generator triggers a resample operation, drawing a new anchor from the Strategy Scheduler’s Top- K distribution and re-attempting the formulation, up to M trials. This mechanism is critical for avoiding diminishing returns. Furthermore, this loop provides an elegant convergence heuristic: if all M trials yield duplicate queries, we declare that the system has reached global convergence.

3) Penalties and Feedback Loop. Beyond producing a valid query, the generator’s final role is to enable system-level learning. Critically, queries result in refusals, empty responses or identified as duplicates incur strategy-specific penalties. This penalty signal is fed back to the scheduler as a reduced payoff, directly influencing its subsequent Empirical Payoff score calculations and anchor selections. This feedback mechanism, which connects the outcome of the generator’s action back to the high-level strategy, allows the system to learn from failed interactions and dynamically adapt its strategy over time.

6. Evaluation

We conduct comprehensive experiments to answer the following research questions:

- **RQ1:** How effective is RAGCRAWLER compared with existing methods?
- **RQ2:** How does the the retriever in victim RAG affect coverage performance?
- **RQ3:** How does the internal LLM agent within attack method influence performance?
- **RQ4:** How robust is the attack against RAG variants employing query rewriting or multi-query retrieval?
- **RQ5:** How do the hyperparameters and each technique affect effectiveness of RAGCRAWLER?

6.1. Evaluation Setup

Dataset. We evaluate on four datasets spanning scientific and medical domains with varying styles and scales. Three datasets, TREC-COVID, SciDocs, and NFCorpus, are drawn from the BEIR benchmark [40], containing about 171.3K, 25.6K, and 5.4K documents, respectively. We further include Healthcare-Magic-100k [41] (abbreviated as Healthcare), with roughly 100K patient-provider Q&A samples. TREC-COVID, SciDocs, NFCorpus, and Healthcare focus on biomedical literature, scientific papers, consumer health, and clinical dialogues, respectively. For efficiency and fair comparison, we randomly select 1,000 de-duplicated documents from each corpus as the victim RAG collection [12], [31]. We confirm that the sampled subsets preserve similar semantic distributions to the full corpora using Energy Distance [42] and the Classifier Two-Sample Test (C2ST) [43], with details in Appendix 9.1.

Generator and Retriever. We employ two retrievers in our evaluations: BGE [44] and GTE [45]. For generators, we evaluate four large language models: Llama 3.1 Instruct-8B (denoted as Llama-3-8B) [46], Command-R-7B [47], Microsoft-Phi-4 [48], and GPT-4o-mini [49]. These generators represent diverse families of reasoning and instruction-tuned models, covering both open-source and proprietary systems and varying parameter scales. The inclusion of GPT-4o-mini, with its built-in safety guardrails [50], demonstrates our attack’s robustness against industry defenses.

Attacker-side LLM. We adopt two attacker-side LLMs to simulate adversarial query generation. In the main experiments, we use Doubao-1.5-lite-32K [51] due to its high speed, cost efficiency, and independence from the RAG’s generator family. This aligns with the black-box assumption. We also evaluate a smaller open-source alternative, Qwen-2.5-7B-Instruct [52], to examine transferability between different model families and sizes.

RAG Setting. We cover three RAG configurations: vanilla RAG, RAG with query rewriting, and RAG employing multi-query retrieval with RRF re-ranking (default: 3 queries per request). We set the retrieval number to $k = 10$ and analyze its impact in Sec. 6.6. The retrieved documents are provided to the generator as contextual input through

a structured system prompt. Further details on the system prompts are provided in Appendix 9.5.

Baselines. We compare RAGCRAWLER against two state-of-the-art black-box RAG extraction attacks: RAGThief [12] and IKEA [11]. RAGThief represents continuation-based attack, and IKEA represents keyword-based attack. To ensure a fair comparison, all attacks employ the same attacker-side LLM. For all experiments, we use the default hyperparameters reported in the original papers. Each attack is allowed to issue at most 1,000 queries to the victim RAG, ensuring consistent query budgets across methods.

Metrics. We evaluate extraction along two axes *coverage* and *content quality*: (i) **Coverage Rate**. This metric quantifies how much of the victim RAG’s private corpus has been exposed through retrieval, corresponding to the adversary’s goal in Eq. 3. Following prior work [11], [12], this metric is only calculated on queries for which the victim RAG produces a *non-refusal* response. (ii) **Semantic Fidelity**. To quantify the semantic overlap between the private corpus \mathcal{D} and the extracted snippets \mathcal{A} , we first measure the similarity for each document $d \in \mathcal{D}$ to its best-aligned snippet using a fixed encoder $E_{\text{eval}}(\cdot)$:

$$s(d) = \max_{e \in \mathcal{E}} \cos(E_{\text{eval}}(d), E_{\text{eval}}(e)). \quad (15)$$

The average of $s(d)$ over the entire corpus represents the overall semantic fidelity of the extracted text. To assess practical utility, we also measure **Reconstruction Fidelity**. We construct a surrogate RAG from the extracted knowledge and evaluate it using the official query sets corresponding to the documents in TREC-COVID, SciDocs, and NFCorpus corpora, totaling 1,860, 2,181, and 1,991 queries, respectively. The Healthcare dataset is excluded due to the absence of official query annotations. We report: (a) Success Rate (fraction of non-refusal responses), (b) Answer Similarity (embedding cosine similarity between surrogate and victim answers); and (c) ROUGE-L score.

6.2. Effectiveness (RQ1)

We evaluate the effectiveness of RAGCRAWLER through three key metrics: corpus coverage rate, semantic fidelity and reconstruction fidelity. Across all evaluations, RAGCRAWLER demonstrates a significant leap in performance over existing baseline attacks.

Coverage Rate. RAGCRAWLER achieves consistently superior extraction efficiency and breadth. As shown in the coverage rate curves in Fig. 8 and Fig. 12, RAGCRAWLER steadily increases the corpus coverage throughout the attack, reaching a final average rate of 66.8% under a 1,000-query budget (Tab. 1). This high efficiency is particularly pronounced in challenging, broad-domain corpora such as SciDocs and TREC-COVID. The success of RAGCRAWLER is attributable to its global knowledge graph and UCB-based planning algorithm. This design enables it to dynamically and strategically traverse the entire semantic space of the corpus, ensuring it continuously targets and extracts from underexplored regions. Furthermore, RAGCRAWLER

TABLE 1: Coverage Rate (CR) and Semantic Fidelity (SF) of attacks across datasets and generators (BGE Retriever). Best results are in **bold**. RAGCRAWLER consistently achieves the highest CR and SF, outperforming baselines across all settings.

Dataset	Generator	Metric	RAGTheif	IKEA	RAGCrawler
TREC-COVID	Llama-3-8B	CR	0.131	0.161	0.494
	Llama-3-8B	SF	0.447	0.495	0.591
	Command-R	CR	0.154	0.173	0.544
	Command-R	SF	0.444	0.525	0.614
SciDocs	Microsoft-Phi-4	CR	0.121	0.197	0.474
	Microsoft-Phi-4	SF	0.468	0.547	0.619
	GPT-4o-mini	CR	0.000	0.197	0.465
	GPT-4o-mini	SF	-	0.543	0.572
NFCorpus	Llama-3-8B	CR	0.053	0.513	0.661
	Llama-3-8B	SF	0.264	0.495	0.523
	Command-R	CR	0.093	0.522	0.717
	Command-R	SF	0.295	0.514	0.561
HealthCare	Microsoft-Phi-4	CR	0.065	0.545	0.711
	Microsoft-Phi-4	SF	0.324	0.534	0.563
	GPT-4o-mini	CR	0.000	0.421	0.516
	GPT-4o-mini	SF	-	0.475	0.492
HealthCare	Llama-3-8B	CR	0.061	0.503	0.797
	Llama-3-8B	SF	0.451	0.644	0.698
	Command-R	CR	0.169	0.517	0.844
	Command-R	SF	0.467	0.656	0.705
HealthCare	Microsoft-Phi-4	CR	0.113	0.566	0.813
	Microsoft-Phi-4	SF	0.487	0.663	0.717
	GPT-4o-mini	CR	0.000	0.493	0.631
	GPT-4o-mini	SF	-	0.631	0.653
HealthCare	Llama-3-8B	CR	0.361	0.687	0.807
	Llama-3-8B	SF	0.536	0.588	0.618
	Command-R	CR	0.170	0.592	0.766
	Command-R	SF	0.383	0.578	0.582
HealthCare	Microsoft-Phi-4	CR	0.052	0.588	0.654
	Microsoft-Phi-4	SF	0.434	0.558	0.599
	GPT-4o-mini	CR	0.000	0.693	0.799
	GPT-4o-mini	SF	-	0.490	0.577

remains highly effective against RAG systems with built-in guardrails (e.g., those using GPT-4o-mini). Its use of stealthy, policy-compliant prompts allows it to circumvent defenses that easily detect and block the explicit jailbreak attempts used by other methods.

In contrast, baseline methods exhibit significant limitations. The strongest baseline, IKEA, plateaus early and achieves an average coverage of only 46.1% (a 20.7 percentage point deficit compared to RAGCRAWLER). RAGThief is even less effective, with an average coverage of a mere 9.6%. These heuristic-based methods tend to repeatedly query semantically similar regions or drift off-topic, failing to achieve comprehensive corpus exploration. RAGThief, in particular, fails completely against guarded models GPT-4o-mini, as its direct jailbreak prompts are consistently refused.

Semantic Fidelity. Beyond extracting a larger volume of content, RAGCRAWLER also ensures the extracted information is of higher quality. RAGCRAWLER achieves the highest Semantic Fidelity (SF) score across all dataset-generator pairs, with a cross-dataset average of 0.605 (Tab. 1). This indicates that the content it extracts is highly faithful to the source documents. This high fidelity is a direct result of our design of the Query Generator, which maintains contextual coherence and ensures that the extracted text chunks are semantically sound and accurate. By comparison,

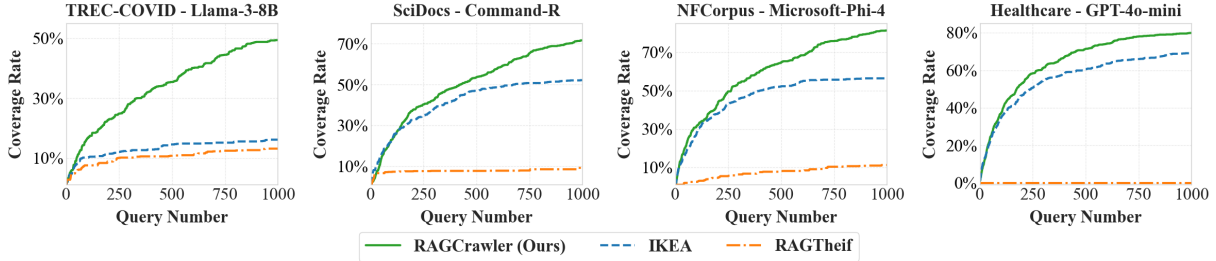


Figure 8: Coverage Rate vs. Query Number (1,000 Budget) across datasets and generators (BGE Retriever). RAGCRAWLER steadily increases coverage and consistently surpasses both RAGTheif and IKEA. Comprehensive results are in Appendix 9.4.

TABLE 2: Reconstruction Fidelity of Surrogate RAG Systems using extracted knowledge (Llama-3-8B Generator, BGE Retriever). Best results are in **bold**. Surrogates built from extracted knowledge of RAGCRAWLER achieve the highest performance in all metrics.

Dataset	Method	SuccessRate	Similarity	Rouge-L
TREC-COVID	RAGTheif	0.1129	0.4920	0.1547
	IKEA	0.2247	0.4779	0.1730
	RAGCrawler	0.3839	0.6098	0.2408
SciDocs	RAGTheif	0.0486	0.4275	0.1131
	IKEA	0.0179	0.4829	0.1277
	RAGCrawler	0.3810	0.5900	0.2285
NFCorpus	RAGTheif	0.0447	0.5156	0.1063
	IKEA	0.4215	0.6064	0.2013
	RAGCrawler	0.5259	0.6992	0.2334

IKEA and RAGTheif score lower, with average SF scores of 0.559 and 0.417, respectively. Their less-targeted query strategies may yield fragmented or contextually distorted content, diminishing the quality of the extracted knowledge.

Reconstruction Fidelity. To assess the practical utility of the extracted knowledge, we measure its effectiveness in a downstream task: building a surrogate RAG system. A surrogate RAG constructed from the knowledge base extracted by RAGCRAWLER demonstrates markedly superior performance. As reported in Tab. 2, it achieves answer success rates ranging from 38.1% to 52.6% on official query sets. Moreover, it obtains the highest scores in embedding similarity (up to 0.699) and ROUGE-L (up to 0.240), confirming the high quality and functional value of the recovered knowledge. This operational effectiveness stems from the comprehensive and semantically integral knowledge base that RAGCRAWLER extracts. In contrast, surrogate systems built from the knowledge extracted by IKEA and RAGTheif perform poorly. This highlights that their extracted content is not only less complete but also less useful for reconstructing the original system’s capabilities.

Takeaway. RAGCRAWLER outperforms prior methods across all datasets and generators, achieving an average coverage rate of 66.8%, compared to 46.1% for IKEA and 9.6% for RAGTheif. It also obtains a superior average semantic fidelity of 0.605. Furthermore, surrogate RAG systems built from its extractions yield the highest answer success rates, confirming that RAGCRAWLER constitutes a more potent and realistic threat to RAG systems.

TABLE 3: Coverage rate (CR) and semantic fidelity (SF) of attacks on RAG using GTE as retriever (Llama-3-8B generator). RAGCRAWLER remains dominant.

Dataset	Metric	RAGTheif	IKEA	RAGCrawler
TREC-COVID	CR	0.191	0.391	0.765
	SF	0.453	0.565	0.610
SciDocs	CR	0.162	0.368	0.833
	SF	0.345	0.495	0.539
NFCorpus	CR	0.386	0.622	0.738
	SF	0.589	0.648	0.671
Healthcare	CR	0.388	0.671	0.728
	SF	0.548	0.576	0.567

6.3. Retriever Sensitivity (RQ2)

To evaluate the robustness of RAGCRAWLER against different retrieval architectures, we evaluated the attack methods on victim RAG systems with GTE [45] as retriever.

RAGCRAWLER demonstrates robustness and adaptability, maintaining its superior performance. As shown in Table 3 for Llama-3-8B generator, RAGCRAWLER achieves an average coverage rate (CR) of 76.6% and a semantic fidelity (SF) of 0.596. Notably, its coverage improves compared to its performance with the BGE retriever (69.0%, from Table 1), showcasing its ability to effectively capitalize on the document set surfaced by any underlying retriever. In contrast, while the baseline methods also see a performance uplift with the GTE retriever (IKEA’s average coverage increases to 53.9% and RAGTheif’s to 28.2%), they still remain far less effective. This indicates that while a different retriever may surface “easier” content for all methods, the heuristic-driven approaches of the baselines are fundamentally less capable of exploiting this opportunity to the same degree as RAGCRAWLER’s strategic exploration.

Takeaway. RAGCRAWLER’s effectiveness is not contingent on a specific retriever. When the victim RAG employs a GTE retriever, RAGCRAWLER achieves an average coverage of 76.6%, substantially outperforming both IKEA (53.9%) and RAGTheif (28.2%). Its strategic, graph-based exploration makes it a more versatile and potent threat across diverse RAG system implementations.

6.4. Agent Sensitivity (RQ3)

To investigate the influence of the attacker’s LLM agent on attack performance, we evaluated the effectiveness with a smaller open-source model, Qwen-2.5-7B-Instruct.

TABLE 4: Coverage rate (CR) and semantic fidelity (SF) of each attacks when using Qwen-2.5-7B-Instruct as attacker’s agent (victim RAG: Llama-3-8B generator, BGE retriever). Best results are in **bold**. RAGCRAWLER continues to attain the highest coverage and fidelity under a smaller model.

Dataset	Metric	RAGTheif	IKEA	RAGCrawler
TREC-COVID	CR	0.271	0.183	0.542
	SF	0.453	0.499	0.610
SciDocs	CR	0.314	0.559	0.675
	SF	0.345	0.495	0.539
NFCorpus	CR	0.386	0.622	0.738
	SF	0.589	0.648	0.671
Healthcare	CR	0.414	0.687	0.799
	SF	0.548	0.576	0.567

RAGCRAWLER demonstrates high effectiveness irrespective of the agent’s scale. Even when powered by the smaller Qwen-2.5-7B-Instruct agent, RAGCRAWLER continues to achieve the highest performance across all metrics, as shown in Table 4. It reaches an average coverage of 68.9% and a semantic fidelity of 0.596, results that are comparable to, and in some cases even exceed, its performance with the larger agent (e.g., 54.2% coverage on TREC-COVID with Qwen vs. 49.4% with Doubao). This resilience stems from our framework’s design, which decouples high-level strategic planning from low-level content generation. The knowledge graph and strategy scheduler dictate the overall attack trajectory, requiring the LLM agent merely to execute localized and well-defined sub-tasks.

In comparison, the baseline methods remain significantly less effective. With the Qwen-2.5-7B-Instruct agent, IKEA achieves an average coverage of 51.3%, while RAGTheif reaches 34.6%. Although RAGTheif sees a slight performance improvement (likely because the constrained divergent ability of smaller model make it less prone to the off-topic drift), it still lags far behind RAGCRAWLER.

Takeaway. The effectiveness of RAGCRAWLER is largely independent of the LLM agent. When using a smaller model such as Qwen-2.5-7B-Instruct, it achieves an average coverage of 68.9%, decisively outperforming baselines. This highlights that the primary strength of our attack lies in its strategic planning, not the raw capability of agent model.

6.5. Defense Robustness (RQ4)

To further explore potential defenses, we extend our evaluation beyond the test against GPT-4o-mini’s built-in guardrails (Sec. 6.2) to two practical mechanisms widely adopted by RAG: query rewriting and multi-query retrieval.

Query Rewriting. In this configuration, the victim RAG system employs an LLM to rewrite incoming queries, aiming to clarify user intent and neutralize potential adversarial patterns before retrieval and generation. RAGCRAWLER exhibits exceptional resilience against this defense, maintaining superior performance metrics. As detailed in Table 5, RAGCRAWLER achieves an average coverage rate of 74.1% and semantic fidelity of 0.591. Although intended as a safeguard, the query rewriting process is paradoxically exploited by our method to enhance extraction. By explicitly refining

the query’s semantic intent, the rewriter enables the retriever to surface a more relevant and diverse set of documents than the original input would yield. RAGCRAWLER’s adaptive planner capitalizes on this context to accelerate corpus exploration; for instance, on the NFCorpus dataset, coverage increases from 73.8% to 85.4% when this defense is active.

In contrast, baseline methods fail to effectively exploit this dynamic. While RAGTheif sees its average coverage improve to 57.9% and IKEA reaches 46.7%, both remain significantly behind RAGCRAWLER. RAGTheif benefits incidentally, as the rewriting step strips away its obvious adversarial suffixes; however, lacking a strategic framework to systematically capitalize on the enhanced retrieval results, it cannot match RAGCRAWLER’s efficiency, underscoring the fundamental limitations of heuristic-based approaches.

Multi-query Retrieval. We next evaluate against multi-query retrieval, which expands each query into several variants whose retrieved results are re-ranked and fused, a process that can influence attack surface. Once again, RAGCRAWLER excels, achieving the highest average coverage of 69.5% and a semantic fidelity of 0.593 (Table 6). This mechanism provides the attacker with a more diverse set of retrieved documents from different semantic clusters. The global graph in RAGCRAWLER is uniquely positioned to exploit this; it integrates this diverse information to build a more comprehensive map of the corpus, thereby generating more effective and far-reaching follow-up queries.

The baseline methods, however, are not equipped to fully leverage this enriched context. IKEA and RAGTheif attain coverage rates of 46.1% and 40.8%, respectively. Their localized strategies are unable to fully synthesize the information from the multiple retrieval results.

Takeaway. RAGCRAWLER remains highly effective against practical RAG defenses. The results demonstrate that common defenses designed to sanitize inputs or strengthen retrieval can be subverted by a strategic attacker and may even amplify the extraction threat, highlighting the need for more advanced safeguards.

6.6. Ablation Study (RQ5)

We first study the influence of score cache and victim retrieval depth. More ablations on modules and hyperparameter choices are provided in Appendix 9.3.

TABLE 5: Coverage rate (CR) and semantic fidelity (SF) of attacks under *query rewriting* (victim RAG: Llama-3-8B generator, BGE retriever). Best results are in **bold**. RAGCRAWLER still achieves the highest coverage and fidelity in this setting, indicating resilience to *query rewriting*.

Dataset	Metric	RAGTheif	IKEA	RAGCrawler
TREC-COVID	CR	0.381	0.241	0.601
	SF	0.519	0.537	0.591
SciDocs	CR	0.561	0.542	0.743
	SF	0.442	0.479	0.507
NFCorpus	CR	0.664	0.489	0.854
	SF	0.633	0.618	0.687
Healthcare	CR	0.709	0.595	0.767
	SF	0.556	0.564	0.577

TABLE 6: Coverage rate (CR) and semantic fidelity (SF) of attacks under *multi-query retrieval* (victim RAG: Llama-3-8B generator, BGE retriever). Best results are in **bold**. RAGCRAWLER still achieves the highest coverage and fidelity, indicating resilience to *multi-query retrieval*.

Dataset	Metric	RAGTheif	IKEA	RAGCrawler
TREC-COVID	CR	0.326	0.189	0.474
	SF	0.525	0.523	0.581
SciDocs	CR	0.352	0.508	0.697
	SF	0.364	0.494	0.514
NFCorpus	CR	0.392	0.540	0.849
	SF	0.588	0.631	0.692
Healthcare	CR	0.562	0.605	0.761
	SF	0.569	0.580	0.587

Score Cache. The Strategy Scheduler module includes a score cache to avoid redundant computations of the CMG for similar states. We measured the impact of this optimization on computational overhead. As shown in Fig. 9, across the evaluated datasets the attacker would need to update over 1.67 million scoring operations without caching, versus only about 0.63 million with our cache (a 62% reduction in workload). In practice, this translates to a faster attack runtime and lower cost, enabling the attacker to scale to larger corpora or tighter time budgets. The benefit of caching grows with the number of queries, since later attack rounds re-use many of the same entity-relation state components.

Victim Retrieval Depth. We also analyzed sensitivity of RAGCRAWLER to the victim RAG’s retrieval depth (k), the number of documents retrieved per query. As illustrated in Fig. 10 for the TREC-COVID dataset, a larger k allows the attacker to acquire knowledge more rapidly; for instance, coverage within 1,000 queries increases from approximately 28% at $k=5$ to over 60% at $k=20$. However, this effect is subject to diminishing returns. As k grows, the additional documents retrieved are increasingly likely to have semantic overlap with previously seen content, providing less novel information for the planner to exploit.

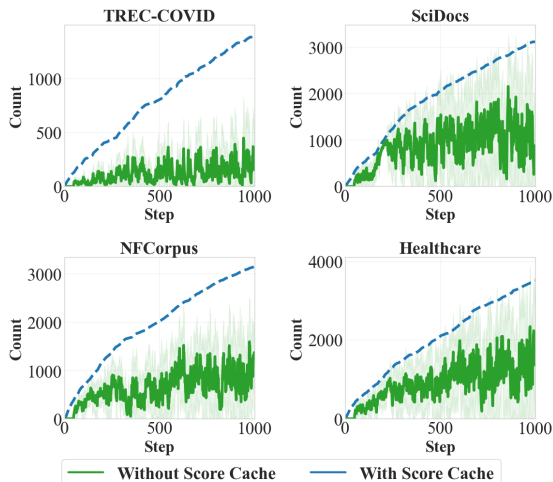


Figure 9: Score Computations with vs. without Caching. Caching reduces the number of similarity score updates by $\sim 2.67 \times$ on average, greatly improving efficiency.

7. Discussion and Related Work

Cost Analysis. RAGCRAWLER is highly cost-effective, with a monetary cost of only \$0.33–\$0.53 per dataset (Tab. 8) and is reducible to **near-zero** using open-source models (Sec. 6.4). This minimal expenditure creates a stark economic asymmetry against the high development costs of victim RAG systems [53]. This asymmetry poses a dual threat: enabling low-cost service piracy by reconstructing the knowledge base (Tab. 2) and exposing victims to severe legal and privacy liabilities under regulations like HIPAA and GDPR if sensitive data is exfiltrated [8], [19].

Defenses. Our attack highlights the inherent limitations of defenses that rely on analyzing queries in isolation. Its use of individually benign queries makes it difficult to counter with conventional tools like guardrails or query rewriting without significant performance penalties. The core challenge is that the malicious pattern is an emergent property of the entire interaction sequence, not an attribute of any single query. This exposes a critical blind spot in static security models and argues for a pivot towards dynamic, behavior-aware defenses. Based on this analysis, we believe query provenance analysis [54], [55], [56], [57] holds significant promise. Because this technique is designed to track relationships across entire sequences, it is theoretically capable of identifying the progressive, goal-oriented patterns of an extraction attack. Verifying its practical effectiveness would be a valuable next step for the research community.

Security Risks in RAG. This paper concentrates on Data Extraction Attacks against RAG systems, where an adversary queries the system to steal or reconstruct its private knowledge base [7], [11], [12], [30], [31]. RAG systems are also susceptible to other security risks [10], [58]. Membership Inference Attacks (MIA) enable an adversary to determine if a specific document is present in the private corpus, thereby exposing the existence of sensitive records [59], [60], [61], [62]. Furthermore, in Corpus Poisoning attacks, an adversary injects malicious data into the RAG knowledge base [63], [64], [65], [66]. Retrieval of this corrupted data can manipulate the system’s output, allowing the attacker to propagate misinformation or harmful content.

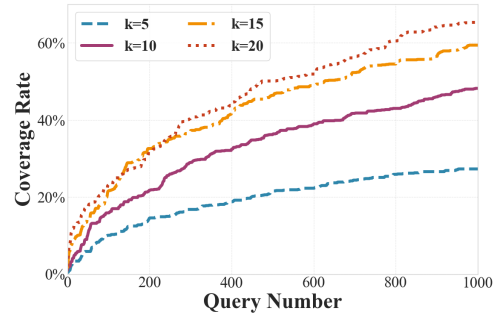


Figure 10: Coverage Rate vs. Query Number for different victim depth k on TREC-COVID, Llama-3-8B, BGE.

8. Conclusion

In this work, we formalized the critical privacy risk of data extraction from RAG systems as an adaptive stochastic coverage problem. We introduced RAGCRAWLER, a novel attack framework that builds a knowledge graph to track revealed information. Our comprehensive experiments demonstrated that RAGCRAWLER significantly outperforms all baselines, achieving up to 84.4% corpus coverage within a fixed query budget. Furthermore, it shows remarkable robustness against advanced RAG that employs query rewriting and multi-query retrieval. Our findings expose a fundamental vulnerability in current RAG architectures, underscoring the urgent need for robust safeguards to protect private knowledge bases.

References

- [1] V. Karpukhin, B. Ong, S. Min, P. S. Lewis, L. Wu, S. Edunov, D. Chen, and W.-t. Yih, “Dense passage retrieval for open-domain question answering,” in *EMNLP (1)*, 2020, pp. 6769–6781.
- [2] P. Lewis, E. Perez, A. Piktus, F. Petroni, V. Karpukhin, N. Goyal, H. Kütter, M. Lewis, W.-t. Yih, T. Rocktäschel *et al.*, “Retrieval-augmented generation for knowledge-intensive nlp tasks,” *Advances in neural information processing systems*, vol. 33, pp. 9459–9474, 2020.
- [3] A. Xu, T. Yu, M. Du, P. Gundecha, Y. Guo, X. Zhu, M. Wang, P. Li, and X. Chen, “Generative ai and retrieval-augmented generation (rag) systems for enterprise,” in *Proceedings of the 33rd ACM International Conference on Information and Knowledge Management*, 2024, pp. 5599–5602.
- [4] Y. Al Ghadban, H. Lu, U. Adavi, A. Sharma, S. Gara, N. Das, B. Kumar, R. John, P. Devarasetty, and J. E. Hirst, “Transforming healthcare education: Harnessing large language models for frontline health worker capacity building using retrieval-augmented generation,” *medRxiv*, pp. 2023–12, 2023.
- [5] L. Loukas, I. Stogiannidis, O. Diamantopoulos, P. Malakasiotis, and S. Vassos, “Making llms worth every penny: Resource-limited text classification in banking,” in *Proceedings of the Fourth ACM International Conference on AI in Finance*, 2023, pp. 392–400.
- [6] S. Zeng, J. Zhang, P. He, Y. Liu, Y. Xing, H. Xu, J. Ren, Y. Chang, S. Wang, D. Yin *et al.*, “The good and the bad: Exploring privacy issues in retrieval-augmented generation (rag),” in *ACL (Findings)*, 2024.
- [7] Z. Qi, H. Zhang, E. P. Xing, S. M. Kakade, and H. Lakkaraju, “Follow my instruction and spill the beans: Scalable data extraction from retrieval-augmented generation systems,” in *The Thirteenth International Conference on Learning Representations*.
- [8] P. Voigt and A. Von dem Bussche, “The eu general data protection regulation (gdpr),” *A practical guide, 1st ed.*, Cham: Springer International Publishing, vol. 10, no. 3152676, pp. 10–5555, 2017.
- [9] G. J. Annas, “Hipaa regulations—a new era of medical-record privacy?” pp. 1486–1490, 2003.
- [10] The Lasso Team. (2024) Rag security: Risks and mitigation strategies. See section: “Security Risks at Retrieval Stage”. [Online]. Available: <https://www.lasso.security/blog/rag-security>
- [11] Y. Wang, W. Qu, Y. Jiang, Z. Liu, Y. Liu, S. Zhai, Y. Dong, and J. Zhang, “Silent leaks: Implicit knowledge extraction attack on rag systems through benign queries,” *arXiv preprint arXiv:2505.15420*, 2025.
- [12] C. Jiang, X. Pan, G. Hong, C. Bao, and M. Yang, “Rag-thief: Scalable extraction of private data from retrieval-augmented generation applications with agent-based attacks,” *arXiv preprint arXiv:2411.14110*, 2024.
- [13] G. L. Nemhauser, L. A. Wolsey, and M. L. Fisher, “An analysis of approximations for maximizing submodular set functions—i,” *Mathematical programming*, vol. 14, no. 1, pp. 265–294, 1978.
- [14] L. A. Wolsey, “An analysis of the greedy algorithm for the submodular set covering problem,” *Combinatorica*, vol. 2, no. 4, pp. 385–393, 1982.
- [15] D. Golovin and A. Krause, “Adaptive submodularity: Theory and applications in active learning and stochastic optimization,” *Journal of Artificial Intelligence Research*, vol. 42, pp. 427–486, 2011.
- [16] A. Narayanan and V. Shmatikov, “Robust de-anonymization of large sparse datasets,” in *2008 IEEE Symposium on Security and Privacy (sp 2008)*. IEEE, 2008, pp. 111–125.
- [17] L. Sweeney, “Simple demographics often identify people uniquely,” *Health (San Francisco)*, vol. 671, no. 2000, pp. 1–34, 2000.
- [18] Y. Cai, Z. Zhang, M. Yao, J. Liu, X. Zhao, X. Fu, R. Li, Z. Liu, X. Chen, Y. Guo *et al.*, “I can tell your secrets: Inferring privacy attributes from mini-app interaction history in super-apps,” in *34th USENIX Security Symposium (USENIX Security 25)*, 2025, pp. 6541–6560.
- [19] S.-C. Lin, J.-H. Yang, R. Nogueira, M.-F. Tsai, C.-J. Wang, and J. Lin, “Conversational question reformulation via sequence-to-sequence architectures and pretrained language models,” *arXiv preprint arXiv:2004.01909*, 2020.
- [20] X. Ma, Y. Gong, P. He, N. Duan *et al.*, “Query rewriting in retrieval-augmented large language models,” in *The 2023 Conference on Empirical Methods in Natural Language Processing*, 2023.
- [21] F. Mo, K. Mao, Y. Zhu, Y. Wu, K. Huang, and J.-Y. Nie, “Convqqr: Generative query reformulation for conversational search,” *arXiv preprint arXiv:2305.15645*, 2023.
- [22] Y. Wang, H. Zhang, L. Pang, B. Guo, H. Zheng, and Z. Zheng, “Maferw: Query rewriting with multi-aspect feedbacks for retrieval-augmented large language models,” in *Proceedings of the AAAI Conference on Artificial Intelligence*, vol. 39, no. 24, 2025, pp. 25434–25442.
- [23] Langchain, “Advanced rag techniques,” <https://langchain-tutorials.com/lessons/rag-applications/lesson-14>, 2025, accessed: 2025-11-04.
- [24] Z. Li, J. Wang, Z. Jiang, H. Mao, Z. Chen, J. Du, Y. Zhang, F. Zhang, D. Zhang, and Y. Liu, “Dmqr-rag: Diverse multi-query rewriting for rag,” *arXiv preprint arXiv:2411.13154*, 2024.
- [25] G. V. Cormack, C. L. Clarke, and S. Buettcher, “Reciprocal rank fusion outperforms condorcet and individual rank learning methods,” in *Proceedings of the 32nd international ACM SIGIR conference on Research and development in information retrieval*, 2009, pp. 758–759.
- [26] A. Krause and C. Guestrin, “Near-optimal observation selection using submodular functions,” in *AAAI*, vol. 7, 2007, pp. 1650–1654.
- [27] S. Khuller, A. Moss, and J. S. Naor, “The budgeted maximum coverage problem,” *Information processing letters*, vol. 70, no. 1, pp. 39–45, 1999.
- [28] S. Ji, S. Pan, E. Cambria, P. Marttinen, and P. S. Yu, “A survey on knowledge graphs: Representation, acquisition, and applications,” *IEEE transactions on neural networks and learning systems*, vol. 33, no. 2, pp. 494–514, 2021.
- [29] A. Beck, “Raising the bar for rag excellence: query rewriting and new semantic ranker,” <https://techcommunity.microsoft.com/blog/azu-re-ai-servicesblog/raising-the-bar-for-rag-excellence-query-rewriting-and-new-semanticranker/4302729/>, 2025, accessed: 2025-11-04.
- [30] S. Cohen, R. Bitton, and B. Nassi, “Unleashing worms and extracting data: Escalating the outcome of attacks against rag-based inference in scale and severity using jailbreaking,” *arXiv preprint arXiv:2409.08045*, 2024.

[31] C. Di Maio, C. Cosci, M. Maggini, V. Poggioni, and S. Melacci, “Pirates of the rag: Adaptively attacking llms to leak knowledge bases,” *arXiv preprint arXiv:2412.18295*, 2024.

[32] A. Yates, M. Banko, M. Broadhead, M. J. Cafarella, O. Etzioni, and S. Soderland, “Textrunner: open information extraction on the web,” in *Proceedings of Human Language Technologies: The Annual Conference of the North American Chapter of the Association for Computational Linguistics (NAACL-HLT)*, 2007, pp. 25–26.

[33] G. Stanovsky, J. Michael, L. Zettlemoyer, and I. Dagan, “Supervised open information extraction,” in *Proceedings of the 2018 Conference of the North American Chapter of the Association for Computational Linguistics: Human Language Technologies, Volume 1 (Long Papers)*, 2018, pp. 885–895.

[34] A. Papaluca, D. Krefl, S. R. Méndez, A. Lensky, and H. Suominen, “Zero-and few-shots knowledge graph triplet extraction with large language models,” in *Proceedings of the 1st workshop on knowledge graphs and large language models (kaLLM 2024)*, 2024, pp. 12–23.

[35] H. Bian, “Llm-empowered knowledge graph construction: A survey,” *arXiv preprint arXiv:2510.20345*, 2025.

[36] D. Edge, H. Trinh, N. Cheng, J. Bradley, A. Chao, A. Mody, S. Truitt, D. Metropolitansky, R. O. Ness, and J. Larson, “From local to global: A graph rag approach to query-focused summarization,” *arXiv preprint arXiv:2404.16130*, 2024.

[37] Z. Guo, L. Xia, Y. Yu, T. Ao, and C. Huang, “Lightrag: Simple and fast retrieval-augmented generation,” *arXiv preprint arXiv:2410.05779*, 2024.

[38] E. Kaufmann, O. Cappé, and A. Garivier, “On bayesian upper confidence bounds for bandit problems,” in *Artificial intelligence and statistics*. PMLR, 2012, pp. 592–600.

[39] P. Auer, N. Cesa-Bianchi, and P. Fischer, “Finite-time analysis of the multiarmed bandit problem,” *Machine learning*, vol. 47, no. 2, pp. 235–256, 2002.

[40] N. Thakur, N. Reimers, A. Rücklé, A. Srivastava, and I. Gurevych, “Beir: A heterogenous benchmark for zero-shot evaluation of information retrieval models,” *arXiv preprint arXiv:2104.08663*, 2021.

[41] L. AI, “Chatdoctor-healthcaremagic-100k,” <https://huggingface.co/datasets/lavita/ChatDoctor-HealthCareMagic-100k>, 2024, dataset on Hugging Face.

[42] G. J. Székely and M. L. Rizzo, “Energy statistics: A class of statistics based on distances,” *Journal of statistical planning and inference*, vol. 143, no. 8, pp. 1249–1272, 2013.

[43] D. Lopez-Paz and M. Oquab, “Revisiting classifier two-sample tests,” *arXiv preprint arXiv:1610.06545*, 2016.

[44] P. Zhang, S. Xiao, Z. Liu, Z. Dou, and J.-Y. Nie, “Retrieve anything to augment large language models,” *arXiv preprint arXiv:2310.07554*, 2023.

[45] Z. Li, X. Zhang, Y. Zhang, D. Long, P. Xie, and M. Zhang, “Towards general text embeddings with multi-stage contrastive learning,” *arXiv preprint arXiv:2308.03281*, 2023.

[46] A. Dubey, A. Jauhri, A. Pandey, A. Kadian, A. Al-Dahle, A. Letman, A. Mathur, A. Schelten, A. Yang, A. Fan *et al.*, “The llama 3 herd of models,” *arXiv e-prints*, pp. arXiv-2407, 2024.

[47] C. F. AI, “C4ai-command-r7b-12-2024,” <https://huggingface.co/CohereForAI/c4ai-command-r7b-12-2024>, 2024, open-source large-language model.

[48] M. Abdin, J. Aneja, H. Behl, S. Bubeck, R. Eldan, S. Gunasekar, M. Harrison, R. J. Hewett, M. Javaheripi, P. Kauffmann *et al.*, “Phi-4 technical report,” *arXiv preprint arXiv:2412.08905*, 2024.

[49] OpenAI, “Gpt-4o mini,” <https://openai.com/index/gpt-4o-mini-advancing-cost-efficient-intelligence/>, 2024, a cost-efficient, small-scale multimodal model from OpenAI.

[50] ———, “Openai safety update: Sharing our practices as part of the ai seoul summit,” <https://openai.com/index/openai-safety-update>, May 2024, accessed: 2025-11-12.

[51] ByteDance, “Doubao-1.5-lite-32k,” <https://www.volcengine.com/doc/s/82379/1554679>, 2024, lightweight version of the Doubao-1.5 series by ByteDance.

[52] Qwen, “Qwen2.5-7b-instruct,” <https://huggingface.co/Qwen/Qwen2.5-7B-Instruct>, 2024, open-source large-language model.

[53] ADaSci Research, “How to evaluate the rag pipeline cost,” <https://adasci.org/how-to-evaluate-the-rag-pipeline-cost>, 2024, accessed: 2025-11-11.

[54] S. Li, Z. Zhang, H. Jia, Y. Guo, X. Chen, and D. Li, “Query provenance analysis: Efficient and robust defense against query-based black-box attacks,” in *2025 IEEE Symposium on Security and Privacy (SP)*. IEEE, 2025, pp. 1641–1656.

[55] X. Han, T. Pasquier, A. Bates, J. Mickens, and M. Seltzer, “Unicorn: Runtime provenance-based detector for advanced persistent threats,” in *27th Annual Network and Distributed System Security Symposium, NDSS 2020*. The Internet Society, 2020.

[56] S. Li, F. Dong, X. Xiao, H. Wang, F. Shao, J. Chen, Y. Guo, X. Chen, and D. Li, “Nodlink: An online system for fine-grained apt attack detection and investigation,” *arXiv preprint arXiv:2311.02331*, 2023.

[57] S. M. Milajerdi, R. Gjomemo, B. Eshete, R. Sekar, and V. Venkatakrishnan, “Holmes: real-time apt detection through correlation of suspicious information flows,” in *2019 IEEE symposium on security and privacy (SP)*. IEEE, 2019, pp. 1137–1152.

[58] B. Ni, Z. Liu, L. Wang, Y. Lei, Y. Zhao, X. Cheng, Q. Zeng, L. Dong, Y. Xia, K. Kenthapadi *et al.*, “Towards trustworthy retrieval augmented generation for large language models: A survey,” *arXiv preprint arXiv:2502.06872*, 2025.

[59] M. Liu, S. Zhang, and C. Long, “Mask-based membership inference attacks for retrieval-augmented generation,” in *Proceedings of the ACM on Web Conference 2025*, 2025, pp. 2894–2907.

[60] A. Naseh, Y. Peng, A. Suri, H. Chaudhari, A. Oprea, and A. Houmansadr, “Riddle me this! stealthy membership inference for retrieval-augmented generation,” *arXiv preprint arXiv:2502.00306*, 2025.

[61] M. Anderson, G. Amit, and A. Goldstein, “Is my data in your retrieval database? membership inference attacks against retrieval augmented generation,” in *International Conference on Information Systems Security and Privacy*, vol. 2. Science and Technology Publications, Lda, 2025, pp. 474–485.

[62] K. Feng, G. Zhang, H. Tian, H. Xu, Y. Zhang, T. Zhu, M. Ding, and B. Liu, “Ragleak: Membership inference attacks on rag-based large language models,” in *Australasian Conference on Information Security and Privacy*. Springer, 2025, pp. 147–166.

[63] W. Zou, R. Geng, B. Wang, and J. Jia, “{PoisonedRAG}: Knowledge corruption attacks to {Retrieval-Augmented} generation of large language models,” in *34th USENIX Security Symposium (USENIX Security 25)*, 2025, pp. 3827–3844.

[64] H. Chaudhari, G. Severi, J. Abascal, M. Jagielski, C. A. Choquette-Choo, M. Nasr, C. Nita-Rotaru, and A. Oprea, “Phantom: General trigger attacks on retrieval augmented language generation,” *arXiv preprint arXiv:2405.20485*, 2024.

[65] S. Cho, S. Jeong, J. Seo, T. Hwang, and J. C. Park, “Typos that broke the rag’s back: Genetic attack on rag pipeline by simulating documents in the wild via low-level perturbations,” in *Proceedings of the 2024 Conference on Empirical Methods in Natural Language Processing (EMNLP 2024)*. Association for Computational Linguistics, 2024.

[66] A. Shafran, R. Schuster, and V. Shmatikov, “Machine against the rag: Jamming retrieval-augmented generation with blocker documents,” *USENIX Security*, 2025.

TABLE 7: Semantic distribution similarity between each full corpus and its 1,000-document sampled subset, measured by Energy Distance (with permutation test p -value) and the Classifier Two-Sample Test (C2ST, using AUC). A small Energy Distance with a high p -value and an AUC near 0.5 indicate distributional similarity.

Corpus	Energy Distance (value / p)	C2ST (AUC)
TREC-COVID	0.0349 / 0.5249	0.4993
SciDocs	0.0329 / 0.5781	0.4938
NFCorpus	0.0281 / 0.6412	0.5053
Healthcare	0.0276 / 0.5947	0.4679

9. Appendix

9.1. Sample Distribution Validation

To ensure that our 1,000-document samples are representative of the full corpora, we compare their semantic distributions using Energy Distance [42] and the Classifier Two-Sample Test (C2ST) [43].

Energy Distance quantifies the difference between two distributions using Euclidean distances, and is well-suited for high-dimensional or non-Gaussian data. A smaller energy distance with a large permutation test p -value suggests no statistically significant difference between the sampled and full sets. As shown in Table 7, all four corpora yield low distances (around 0.03) and high p -values (> 0.5), indicating strong alignment between samples and full sets. C2ST (Classifier Two-Sample Test) reframes distribution comparison as a binary classification task. If a classifier cannot distinguish between samples and the full corpus ($AUC \approx 0.5$), the two distributions are considered similar. In Table 7, all AUC scores fall within the 0.46–0.51 range, reinforcing that no meaningful distinction can be learned between the subsets and their corresponding full corpora.

9.2. Proof of Theorems

Proof of Theorem 2: Adaptive Monotonicity and Submodularity in RAG Crawling

Proof. (Adaptive Monotonicity) The coverage function $f(S, \Phi)$ is monotone with respect to the query set S . Issuing an additional query q can only increase or preserve the number of unique documents retrieved. That is, for any realization of Φ ,

$$f(S \cup \{q\}, \Phi) \geq f(S, \Phi).$$

Taking the expectation conditioned on ψ preserves this inequality, so $\Delta(q | \psi) \geq 0$.

(Adaptive Submodularity) Suppose ψ' extends ψ , meaning that the attacker has issued more queries and observed more information. Let S and S' denote the corresponding sets of issued queries, where $S \subseteq S'$. Since more of the corpus has potentially been covered under S' , the additional gain from issuing a new query q can only decrease. Formally, for any realization of Φ , we have

$$f(S \cup \{q\}, \Phi) - f(S, \Phi) \geq f(S' \cup \{q\}, \Phi) - f(S', \Phi).$$

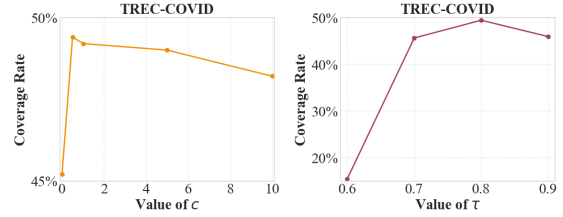


Figure 11: Hyperparameter Choices of RAGCRAWLER.

Taking expectation conditioned on ψ and ψ' respectively, we obtain

$$\Delta(q | \psi) \geq \Delta(q | \psi').$$

□

9.3. Additional Ablations

Modules. The effectiveness of RAGCRAWLER stems from the synergistic integration of its three architectural modules. Without the KG-Constructor, the system loses its global state memory, becoming a stateless, reactive loop unable to distinguish explored regions, a behavior characteristic of IKEA. Without the Strategy Scheduler, the system cannot perform UCB-based prioritization; a fallback to random anchor selection would mimic IKEA’s keyword-based strategy. Finally, without the Query Generator, the scheduler’s strategic plan cannot be translated into executable queries, rendering the planning moot.

Hyperparameter Choices. We examine two key hyperparameters in RAGCRAWLER: the UCB exploration coefficient c used by the Strategy Scheduler for query selection, and the similarity threshold τ used by the Query Generator to filter high-similarity queries (thereby controlling early stopping). As shown in Fig. 11, a moderate UCB coefficient of $c = 0.5$ delivers the best performance by balancing exploitation and exploration. Increasing or decreasing c from this value noticeably degrades performance, underscoring that $c = 0.5$ is near-optimal for a proper exploration-exploitation trade-off. Similarly, the threshold τ exhibits a clear sweet spot. Setting τ too low often causes premature termination. On the other hand, an overly high threshold produces queries that are not sufficiently distinct from one another, which limits exploration efficiency. Our chosen $\tau = 0.8$ navigates between these extremes.

9.4. Coverage Rate Curves

For completeness, we provide all Coverage Rate curves across datasets and settings for all experiments in Sec 6.2, Sec. 6.3 and Sec. 6.4 in Fig. 12, Fig. 13 and Fig. 14.

9.5. Prompts for Experimental Stages

We document the exact prompts used in RAG settings. More prompts in our method can be found in our code.

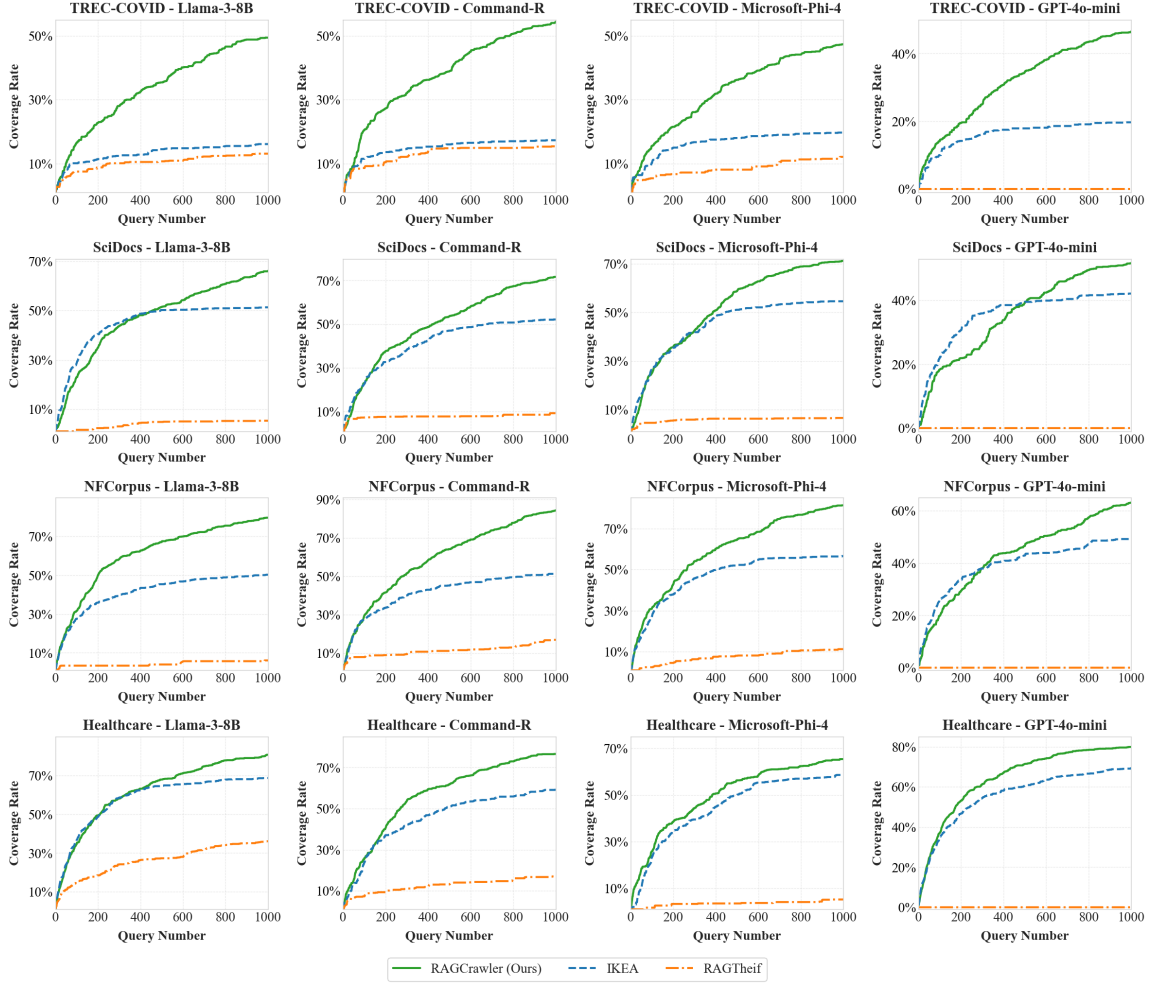


Figure 12: Coverage Rate vs. Query Number (1,000 Budget) across four datasets and four generators.

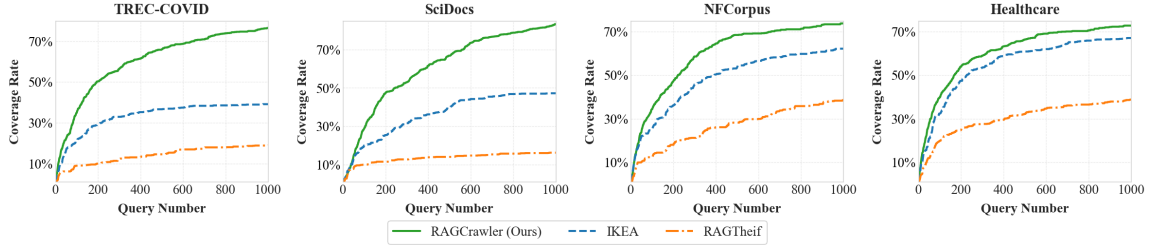


Figure 13: Coverage Rate vs. Query Number (1,000 Budget) across four datasets (GTE Retriever, Llama-3-8B generator).

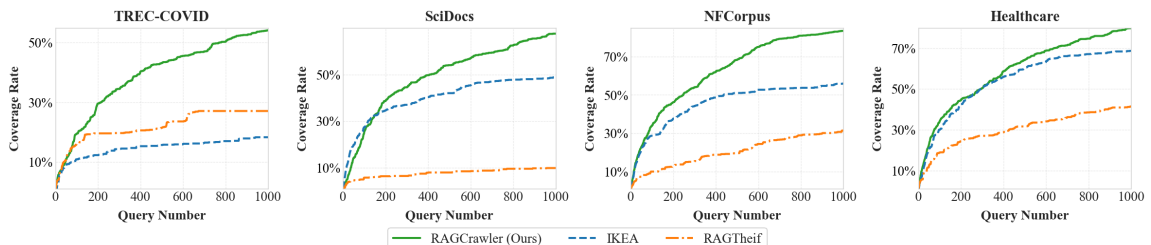


Figure 14: Coverage Rate vs. Query Number (1,000 Budget) across four datasets with Qwen-2.5-7B-Instruct as attacker LLM (BGE Retriever, Llama-3-8B generator).

RAG System Prompt

You are an assistant for question-answering tasks. Use the following pieces of retrieved context to answer the question. If you don't know the answer, say that you don't know.

Context: [context]

Query: [query]

Answer:

Query Rewriting Prompt in RAG System

You are an helpful assistant. Your task is to rewrite the given user question to clarify the user's intent and remove any adversarial intent. Provide directly output the rewritten question without any other text.

Original Question: [query]

Answer:

Multi-query Prompt in RAG System

You are an helpful assistant. Your task is to generate 3 different versions of the given user question to retrieve relevant documents from a vector database. By generating multiple perspectives on the user question, your goal is to help the user overcome some of the limitations of the distance-based similarity search. Provide directly output these alternative questions separated by newlines without any other text.

Original Question: [query]

Answer:

9.6. Cost of the attack

We estimate the cost of executing RAGCRAWLER under realistic conditions. As reported in Table 8, the attacker processes approximately 6–10 million tokens per dataset. Based on Doubao-1.5-lite-32K's API pricing (\$0.042 per million input tokens and \$0.084 per million output tokens), the total cost per attack is remarkably low, i.e., roughly \$0.33 to \$0.53 per dataset. Moreover, as shown in Sec. 6.4, substituting a freely available open-source model such as Qwen-2.5-7B does not degrade the performance of RAGCRAWLER, enabling the attack to be executed at **virtually zero cost**, aside from any fees for the RAG service and GPU hosting.

TABLE 8: Token usage and estimated cost per corpus for KG-Constructor (KG-C) and Query Generator (QG) using Doubao-1.5-lite-32k. “InTok” and “OutTok” denote input and output token counts. Each attack costs under \$1.

Metric	TREC-COVID	SciDocs	NFCorpus	Healthcare
KG-C InTok (M)	5.561	6.209	5.997	9.094
KG-C OutTok (M)	0.724	1.277	1.076	1.373
QG InTok (M)	0.847	0.596	0.366	0.783
QG OutTok (M)	0.042	0.027	0.017	0.035
Total Cost (\$)	0.333	0.395	0.359	0.533

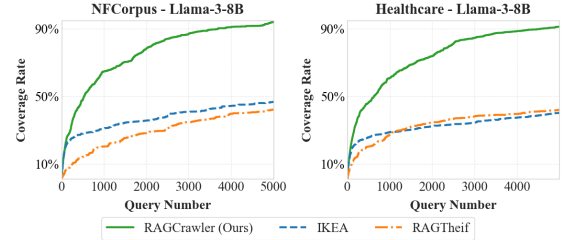


Figure 15: Coverage Rate vs. Query Number (5,000 Budget) on NFCorpus and Healthcare with GPT-4o-mini as attacker LLM (BGE Retriever, Llama-3-8B generator).

9.7. Additional Experiments Results

To further investigate the impact of scale, a complementary study was conducted with an expanded configuration of 2,000 documents and a 5,000-Budget. The coverage rate curves for the NFCorpus and Healthcare datasets from this study are depicted in Fig. 15.